

Arabian Journal of Geosciences

Identification of geochemical anomalies by number-size (N-S) fractal model in Bardaskan area, NE Iran --Manuscript Draft--

Manuscript Number:	AJGS-D-12-00056
Full Title:	Identification of geochemical anomalies by number-size (N-S) fractal model in Bardaskan area, NE Iran
Article Type:	Original Paper
Abstract:	<p>Geochemical anomaly separation and identification using the number-size (N-S) model at Bardaskan area, NE Iran, is studied in this paper. Lithogeochemical data were used in this study which was conducted for the exploration for Au and Cu mineralization and enrichments in Bardaskan area. There are two major mineralization phases concluded epithermal gold and a disseminated systems. N-S Log-log plots for Cu, Au, Sb and As illustrated multifractal natures. Several anomalies at local scale were identified for Au (32 ppb), Cu (28 ppm), As (11 ppm) and Sb (0.8 ppm) the obtained results suggests existence of local Au and Cu anomalies whose magnitude generally is above 158 ppb and 354 ppm, respectively. The most important mineralization events are responsible for presence of Au and Cu at grades above 1778 ppb and 8912 ppm. The study reveals threshold values for Au and Cu are being a consequence of the occurrence of anomalous accumulations of phyllic and silicification alteration zones and metamorphic rocks especially in tuffaceous sandstones and sericite schist types. The obtained results were correlated with fault distribution patterns reveals a positive direct correlation between mineralization in anomalous areas and the faults present in the mineralized system.</p> <p>Keywords: Geochemical anomaly, Epithermal system, Number-size (N-S) model, Multifractal, Bardaskan, NE Iran.</p>

1
2
3
4
5
6
7
8
9
10
11
12
13
14
15
16
17
18
19
20
21
22
23
24
25
26
27
28
29
30
31
32
33
34
35
36
37
38
39
40
41
42
43
44
45
46
47
48
49
50
51
52
53
54
55
56
57
58
59
60
61
62
63
64
65

1 Identification of geochemical anomalies by number-size (N-S) fractal model in

2 Bardaskan area, NE Iran

3 Mehdi Hashemi^{1*}, Iraj Rasa², Musa Noghreian³, Peyman Afzal⁴

4 ¹ Department of Geology, Science and Research branch, Islamic Azad University, Tehran, Iran

5 ² Shahid Beheshti University, Earth Sciences Faculty, Tehran, Iran

6 ³ Isfahan University, Department of Geology, Isfahan, Iran

7 ⁴ Islamic Azad University, Department of Mining Engineering, Tehran, Iran

* Corresponding author: Mehdi Hashemi, E-mail: economic.geology@yahoo.com

1
2
3
4
5
6
7
8
9
10
11
12
13
14
15
16
17
18
19
20
21
22
23
24
25
26
27
28
29
30
31
32
33
34
35
36
37
38
39
40
41
42
43
44
45
46
47
48
49
50
51
52
53
54
55
56
57
58
59
60
61
62
63
64
65

28 1. Introduction

29 Identification and recognition of anomalies from background is an essential issue in geochemical exploration. In the
30 last century, customized statistical methods usually assumed that the concentration of chemical elements in the crust
31 follow a normal or log-normal distribution. A geochemical anomaly as defined is a region where the concentration
32 of a specific element is greater than a certain threshold value by statistical parameters, such as mean, median, mode,
33 and standard deviation (Bolviken et al., 1992; Cheng and Agterberg, 1996; Li et al., 2003). But, statistical methods
34 e.g., by histogram analysis or Q-Q plots assuming normality or lognormality and do not consider the shape, extent
35 and magnitude of anomalous areas and disregarding spatial distribution (Cheng et al., 1994; Agterberg, 1995; Afzal
36 et al., 2010; Deng et al., 2010).

37 Fractal models and methods can be introduced and established by Mandelbrot (1983), which he has applied to
38 objects that were too irregular to be described by ordinary Euclidean geometry (Agterberg et al., 1993; Cheng et al.,
39 1994; Sim et al., 1999; Davis, 2002). Fractal models have been applied to geosciences studies since late 1980s (For
40 example, Turcotte, 1986; Meng and Zhao, 1991; Sim et al., 1991; Cheng et al., 1994; Agterberg et al., 1996; Cheng,
41 1999; Gonclaves et al., 2001; Li et al., 2003; Zuo et al., 2009; Afzal et al., 2010; Carranza and Sadeghi, 2010; Deng
42 et al., 2010; Afzal et al., 2011; Afzal et al., 2012). Mandelbrot (1983) proposed number-size (N-S) model based on
43 the elemental geochemical distributions and occupy number of samples relationships. Agterberg (1995) and Deng et
44 al. (2010) depicted that there are various parameters which have a key role in elemental distributions for a given
45 geological-geochemical environments.

46 In this paper, Cu, Au, As and Sb anomalies are separated and delineated by number-size model in Bardaskan area,
47 NE Iran. Subsequently, a general discussion is argued whereby the anomalous threshold values are correlated to the
48 relevant structural, lithological, and alteration data and this may explain how obtained results were derived.

50 2. The number-size model

51 The N-S model, which was introduced and proposed by Mandelbrot (1983), can be used to describe the elemental
52 distribution without pre-treatment and evaluation of data. The model shows that there is a relationship between
53 desired certain attributes (e.g., ore element in this paper) and their cumulative numbers of samples with those
54 characteristics. Based on the model, Agterberg (1995) proposed a multifractal model named size-grade for
55 determination of the spatial distributions of giant and super-giant mineral deposits. Monecke et al. (2005) utilized

1
2
3
4 56 the N-S model to describe element enrichments associated with metasomatic processes during the formation of
5
6 57 hydrothermal ores in the Waterloo massive sulfide deposit, Australia. The model is expressed by the following
7
8 58 equation (Mandelbrot, 1983; Sanderson et al., 1994; Zou et al., 2009; Deng et al. 2010):
9

10 59
$$N(\geq\rho) = F\rho^{-D} \quad (1)$$

11

12 60 where ρ denotes element concentration, $N(\geq\rho)$ denotes cumulative number of samples with concentration values
13
14 61 greater than or equal to ρ , F is a constant and D is the scaling exponent or fractal dimension of the distribution of
15
16 62 element concentrations. Respect to Mandelbrot (1983) and Deng et al. (2010), log-log plots of $N(\geq\rho)$ versus ρ show
17
18 63 straight line segments with different slopes $-D$ corresponding to certain concentration intervals.
19

20 64

22 65 3. Geological setting of the Bardaskan area

23
24
25 66 The Bardaskan area of about 7.5 km² is situated about 16 km North of Bardaskan in NE Iran (Fig. 1). This
26
27 67 mineralized area is located in Taknar zone, which is one of the subdivisions of Iranian central structural zone at
28
29 68 north Darouneh fault (Alavi, 1994). Bardaskan area includes Au epithermal and Cu disseminated systems
30
31 69 (Babakhani et al., 1999). The study area is mainly comprised of Upper Precambrian volcanic, metamorphic and
32
33 70 volcano-clastics rocks from Taknar zone. Volcanic rocks are included rhyolite, rhyodacite, diabase and spillite.
34
35 71 However, the metamorphic rocks, including meta-sandstone, schist especially sericite schist and chlorite schist, and
36
37 72 slates are existed in the mineralized area. Tuffaceous sandstones and schists are extended in this area (Fig. 1).
38

39 73 The main structural features are two faults system trending NE-SW and E-W. Locally, their feather type fractures
40
41 74 and joints are intense, as illustrated in Fig. 1. The main alteration zones of phyllic, silicification and chloritization
42
43 75 types were accompanied by the quartz-sulfides veins to veinlets fillings of quartz. The ore minerals, specifically
44
45 76 chalcopyrite and pyrite and native Au are present and, the latter ones occurred in the zone of quartz-sulfide veins
46
47 77 and sericite alteration zone, as depicted in Fig. 1. Precise extension and relationships between alteration zones and
48
49 78 mineralization, and economical evaluation of the area are still being investigated and is under study.
50

51 79

53 80 4. Litho geochemistry

54
55
56 81 Total of 483 collected litho geochemical samples were analyzed by ICP-MS for elements which relate to Au and Cu
57
58 82 mineralization and are of interest, and As and Sb concentrations were of no significance. The location map of the
59
60 83 samples' position in the area is depicted in Fig. 2. Statistical results show that Au, Cu, As and Sb mean values are 38
61
62
63
64
65

1
2
3
4 84 ppb, 437, 10.3 and 1.72 ppm, respectively. Their distributions and are not normal and variation between maximum
5
6 85 and minimum for these data show a wide range (Fig. 3).

7
8 86 The elemental grades were sorted out based on decreasing grades and their cumulative numbers. Finally, elemental
9
10 87 log-log plots were generated for Au, Cu, As and Sb, as illustrated in Fig. 4. Based on this procedure, there are 5
11
12 88 geochemical populations for Au, Cu, As and Sb (Fig. 4). Cu anomalous threshold is 28 ppm and its high intensity
13
14 89 anomaly is 8912 ppm. Also, it is obvious that there are four steps of Cu enrichments based on log-log plot, as shown
15
16 90 in Fig. 4.

17
18 91 The first event for Cu N-S variations occurred at grades below 28 ppm. The second event shows up between grades
19
20 92 28 ppm and 354 ppm. The third happen is between 354-8912 ppm for Cu concentration. The final event included
21
22 93 major Cu mineralization which occurred and interpreted in grades higher than 8912 ppm. Au threshold and high
23
24 94 intensity anomalies are 32 ppb, and 1778 ppb, as depicted in Fig. 4. Au log-log plot shows that major Au enrichment
25
26 95 occurred at 158 ppb and higher. As anomalous threshold (as pathfinder of Au) is about 1.6 ppm. There are three
27
28 96 enrichment steps interpreted as seen in N-S log-log plot of Au and As in Fig. 4. Major As enrichment started from
29
30 97 25.1 ppm, and, 177.8 ppm concentration is beginning of high intensity As anomaly. Threshold value of Sb is 0.8
31
32 98 ppm and high intensive Sb anomalous parts have concentrations higher than 12.6 ppm.

33
34 99 Geochemical maps were constructed with IDS (Inverse Distance Squared) method by RockWorks™ v. 15 software
35
36 100 package. The area was gridded by 10 m×10 m cells. Obviously situations of Au anomalies are in northern parts of
37
38 101 the area and the high intensive anomalies are situated in NE parts as depicted in Fig. 5. Moreover, Cu anomalies are
39
40 102 situated in northern, central and southern parts of the area also high intensive Cu anomalies were situated in central
41
42 103 part of the deposit (Fig. 5). Main As and Sb anomalies exist in northern part of the area and correlated with Au
43
44 104 anomalies location, as depicted in Fig. 5.

45
46 105
47
48
49 106 **5. Comparison with geological characteristics**

50
51 107 Thresholds values of elements obtained from N-S model are compared and correlated to specific geological
52
53 108 particulars of the area including considering nature of lithological units, faults and alterations. Au, Cu, As and Sb
54
55 109 distributions in the Bardaskan area, and the faults map are shown in Fig. 6. The anomalous parts visibly show the
56
57 110 main identified faults especially in northern, NE and central parts of the area. Comparison between faults positions
58
59 111 and elemental anomalies shows that faults intersect the anomalies situated near those structures (Fig. 6). Moreover,
60
61
62
63
64
65

1
2
3
4
5
6
7
8
9
10
11
12
13
14
15
16
17
18
19
20
21
22
23
24
25
26
27
28
29
30
31
32
33
34
35
36
37
38
39
40
41
42
43
44
45
46
47
48
49
50
51
52
53
54
55
56
57
58
59
60
61
62
63
64
65

112 faults and elemental anomalies have a proportional relationship. High grade elemental anomalies occurred inside
113 and within the fault zones or situated on faults intersection areas (Fig. 6). This is a positive parameter because
114 silicified and quartz-sulfide veins were occurred along these faults and Au particles are existed in these veins and
115 veinlets.

116 In the area, based on results of the N-S model, the elemental anomalies correlated with different rock types. High
117 amounts of Cu, over 8912 ppm, are highest in sericite and chlorite schists. There are sulfide mineralization
118 especially chalcopyrite. The Au high intensity anomalous parts, higher than 158 ppb, are situated in tuffaceous
119 sandstones. Also there are quartz-sulfide veins and veinlets. An epithermal system is existed in this area and
120 correlated within main Au, As and Sb anomalies. Also, the main step As mineralization, higher than 25 ppm, is
121 correlated within sericite schists as presented in Fig. 7. Alterations have a strong positive relationship with Cu, Au,
122 As and Sb anomalies, especially in northern part of the area. All of the anomalous parts are covered by
123 chloritization, sericitization and silicification alterations. Most chloritization alteration is associated with Cu
124 anomalies (Fig. 7). Cu with concentration at higher than 354 ppm, Au higher than 158 ppb, As higher than 25 ppm,
125 and Sb higher than 12 ppm do have anomalies in northern parts of the area and are covered by chloritization and
126 silicification alterations.

128 6. Conclusions

129 The study on Bardaskan area indicates the potential use of the N-S model for geochemical anomaly separation as a
130 useful tool for geochemical exploration, commonly used in litho-geochemistry. The advantages of the model relies
131 fundamentally on its straightforwardness, and easy computational achievement, as well as the possibility to compute
132 the anomalous threshold values for different elements, which is the most useful criteria for cross examination of
133 information with numerical data from different sources.

134 There exists a proper correlation between the calculated anomalous threshold values and the geological specifics in
135 the Bardaskan area. These results may also be interpreted differently according to their multifractal curves in log-log
136 plots. Cu, Au As and Sb concentrations in the area may be a result of the four steps of enrichment, i.e.,
137 mineralization and later dispersions. Au and Cu log-log plots were shown that there are three steps for their
138 mineralization and dispersion. Major Au mineralization occurred in silicified units in NE parts of the area. Au

1
2
3
4
5
6
7
8
9
10
11
12
13
14
15
16
17
18
19
20
21
22
23
24
25
26
27
28
29
30
31
32
33
34
35
36
37
38
39
40
41
42
43
44
45
46
47
48
49
50
51
52
53
54
55
56
57
58
59
60
61
62
63
64
65

particles are occurred in quartz-sulfide veins and veinlets. Main anomalies of As and Sb are situated in NE part of the area and correlated with main Au anomalies. It can be interpreted that there is an Au epithermal system. The occurrence of Cu higher than 8912 ppm in tuffaceous sandstones and chlorite schists in central parts of the area has been actually realized in the samples collected from the field. The studied elements anomalies have proper and direct relationships with faults in Bardaskan area. High intensity elemental anomalies are mostly located at faults intersections or near to fault zones. It is important because quartz-sulfide veins and veinlets are occurred along these faults. There is a good correlation between chloritization and silicification alterations and anomalous concentration, of Au, Cu, As and Sb. Silicification alteration has good relationships with Au high grade anomalous enrichment parts.

Acknowledgement

Authors would like to thank manager of MadanKav Co. for authorizing the dataset of the Bardaskan area.

References

- Afzal, P., Khakzad, A., Moarefvand, P., Rashidnejad Omran, N., Esfandiari, B., Fadakar Alghalandis, Y., 2010. Geochemical anomaly separation by multifractal modeling in Kahang (Gor Gor) porphyry system, Central Iran, *Journal of Geochemical Exploration* 104, 34–46.
- Afzal, P., Fadakar Alghalandis, Y., Khakzad, A., Moarefvand, P., Rashidnejad Omran, N., 2011. Delineation of mineralization zones in porphyry Cu deposits by fractal concentration–volume modeling, *Journal of Geochemical Exploration* 108, 220–232.
- Afzal, P., Fadakar Alghalandis, Y., Moarefvand, P., Rashidnejad Omran, N., Asadi Haroni, H., 2012. Application of power-spectrum–volume fractal method for detecting hypogene, supergene enrichment, leached and barren zones in Kahang Cu porphyry deposit, Central Iran *Journal of Geochemical Exploration* 112, 131-138.
- Agterberg, F.P., Cheng, Q., Wright, D.F., 1993. Fractal modeling of mineral deposits. In: Elbrond, J., Tang, X. (Eds.), 24th APCOM symposium proceeding, Montreal, Canada, 43–53.
- Agterberg, F.P., 1995. Multifractal modeling of the sizes and grades of giant and supergiant deposits. *International Geology Review* 37, 1–8.
- Agterberg, F.P., Cheng, Q., Brown, A., Good, D., 1996. Multifractal modeling of fractures in the Lac du Bonnet batholith, Manitoba. *Computers and Geosciences* 22 (5), 497–507.
- Alavi, M., 1994. Tectonics of Zagros Orogenic belt of Iran, new data and interpretation. *Tectonophysics* 229, 211 –238 .
- Babakhani, A., Mehrpartu, M., Radfar, J., Majidi, J., 1999, Geological and exploration report of Taknar polymetallic deposit, Iranian Geological survey, Tehran, p. 215.
- Bolviken, B., Stokke, P.R., Feder, J., Jossang, T., 1992. The fractal nature of geochemical landscapes. *Journal of Geochemical Exploration* 43, 91-109.

1
2
3
4 170 Carranza, E.J.M., Sadeghi, M., 2010. Predictive mapping of prospectively and quantitative estimation of undiscovered VMS deposits in
5 171 Skellefte district (Sweden). *Ore Geology Reviews* 38, 219–241.
6
7 172 Cheng, Q., Agterberg, F.P., Ballantyne, S.B., 1994. The separation of geochemical anomalies from background by fractal methods. *Journal of*
8
9 173 *Geochemical Exploration* 51, 109–130.
10
11 174 Cheng, Q., Agterberg, F.P., 1996. Multifractal modeling and spatial statistics. *Math. Geol* 28 (1), 1-16.
12 175 Cheng, Q., 1999. Spatial and scaling modelling for geochemical anomaly separation. *Journal of Geochemical Exploration* 65 (3), 175–194.
13
14 176 Davis, J. C., 2002. *Statistics and Data Analysis in Geology*, 3th ed. John Wiley & Sons Inc, New York.
15 177 Deng, J., Wang, Q., Yang, L., Wang, Y., Gong, Q., Liu, H., 2010. Delineation and explanation of geochemical anomalies using fractal models
16
17 178 in the Heqing area, Yunnan Province, China. *Journal of Geochemical Exploration* 105, 95-105.
18
19 179 Goncalves, M. A., Mateus, A., Oliveira, V., 2001. Geochemical anomaly separation by multifractal modeling. *Journal of Geochemical*
20 180 *Exploration* 72, 91-114.
21
22 181 Li, C., Ma, T., Shi, J., 2003. Application of a fractal method relating concentrations and distances for separation of geochemical anomalies
23 182 from background. *Journal of Geochemical Exploration* 77, 167–175.
24
25 183 Mandelbrot, B.B., 1983. *The Fractal Geometry of Nature*. W. H. Freeman, San Fransisco. 468 pp.
26
27 184 Meng, X., Zhao, P., 1991. Fractal method for statistical analysis of geological data. *Chinese Journal of Geosciences* 2, 207–211.
28
29 185 Monecke, T., Monecke, J., Herzig, P.M., Gemmel, J.B., Monch, W., 2005. Truncated fractal frequency distribution of element abundance data:
30 186 A dynamic model for the metasomatic enrichment of base and precious metals. *Earth and Planetary Science Letters* 232, 363- 378.
31
32 187 Sanderson, D.J., Roberts, S., Gumiel, P., 1994. A Fractal relationship between vein thickness and gold grade in drill core from La Codosera,
33 188 Spain. *Economic Geology* 89, 168–173.
34
35 189 Sim, B.L., Agterberg, F.P., Beaudry, C., 1999. Determining the cutoff between background and relative base metal contamination levels using
36 190 multifractal methods. *Computers & Geosciences* 25, 1023–1041.
37
38 191 Turcotte, D.L., 1986. A fractal approach to the relationship between ore grade and tonnage. *Economic Geology* 18, 1525–1532.
39
40 192 Zuo, R., Cheng, Q., Xia, Q., 2009. Application of fractal models to characterization of vertical distribution of geochemical element
41 193 concentration, *Journal of Geochemical Exploration* 102(1), 37-43.
42
43 194
44
45 195
46
47
48
49
50
51
52
53
54
55
56
57
58
59
60
61
62
63
64
65

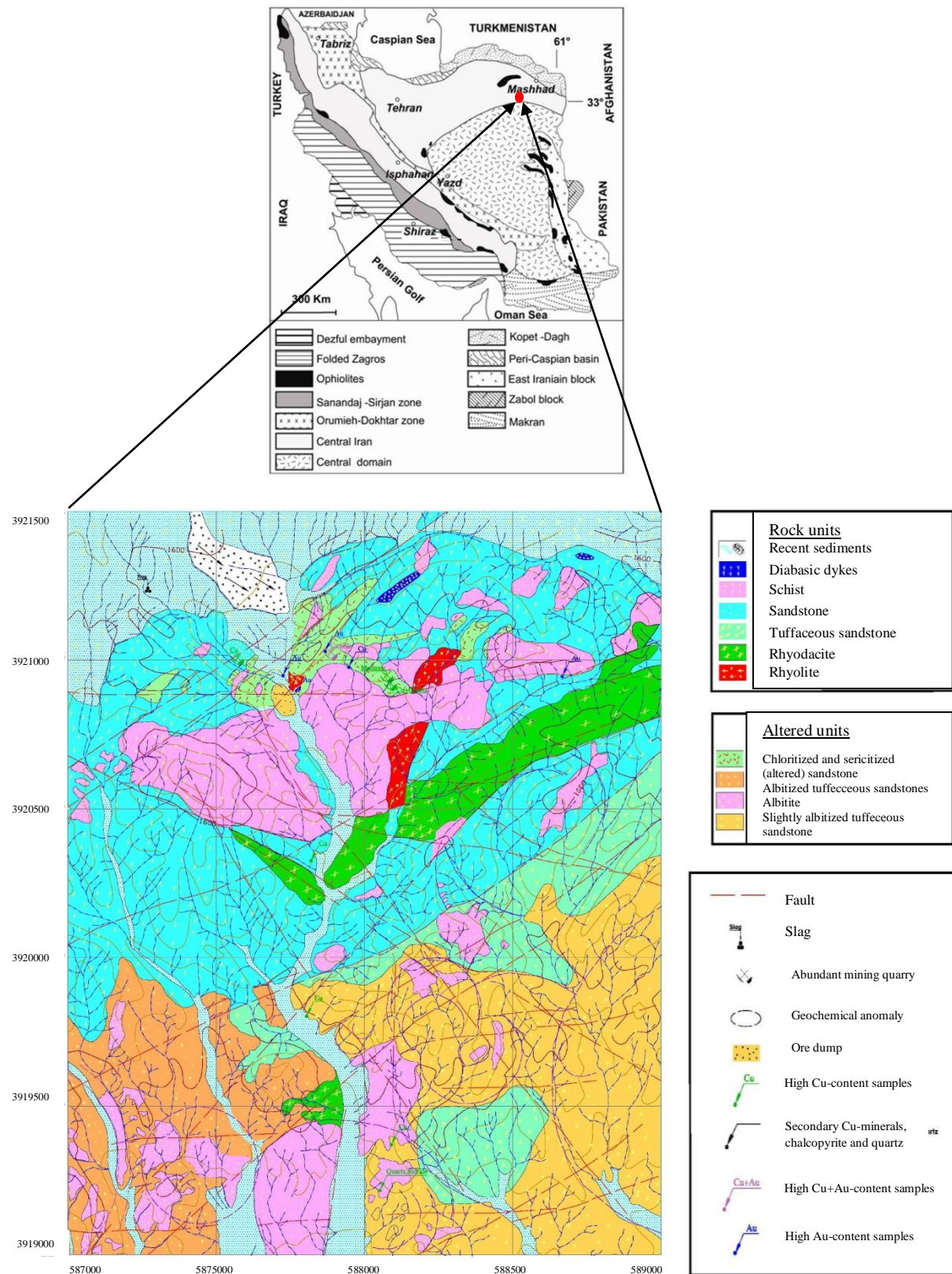


Fig. 1. Location of Bardaskan area in Iranian structural map (Alavi, 1994) and Geological map of the area.

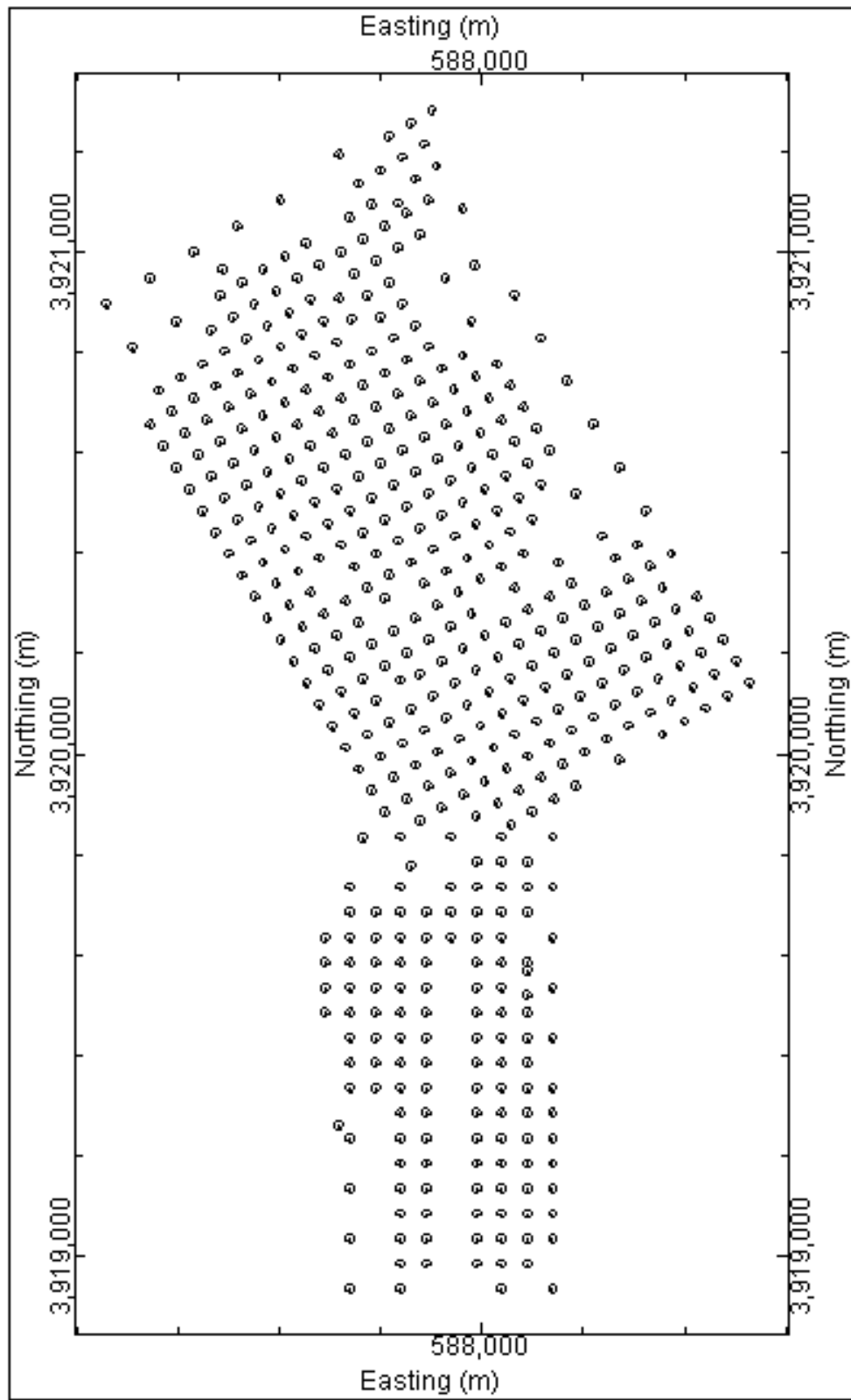


Figure 2. Lithochemical samples location map of Bardaskan area

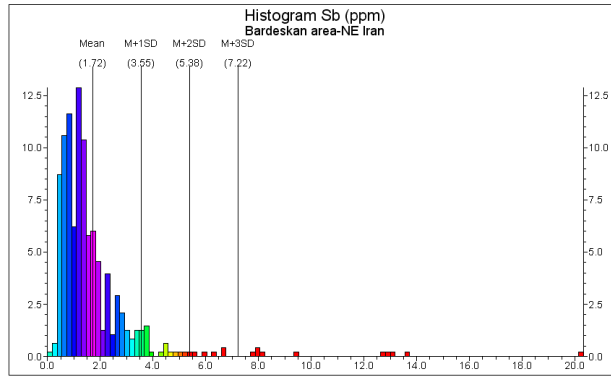
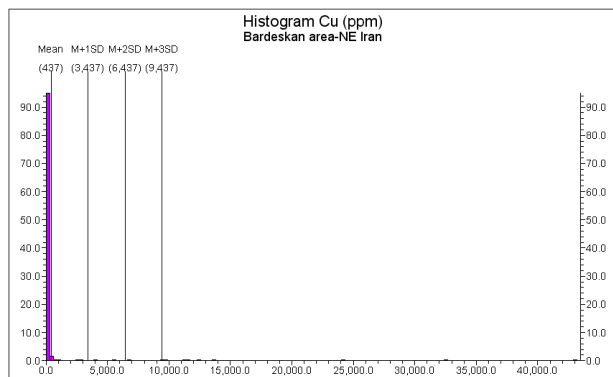
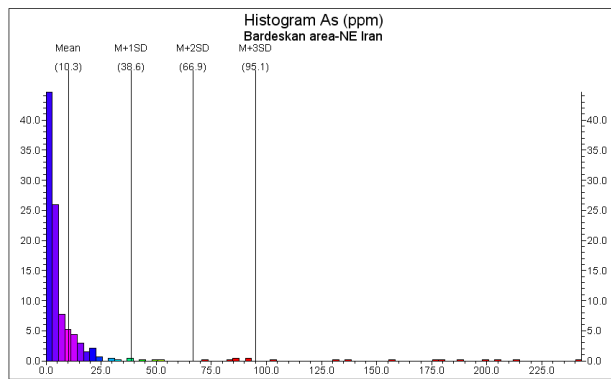
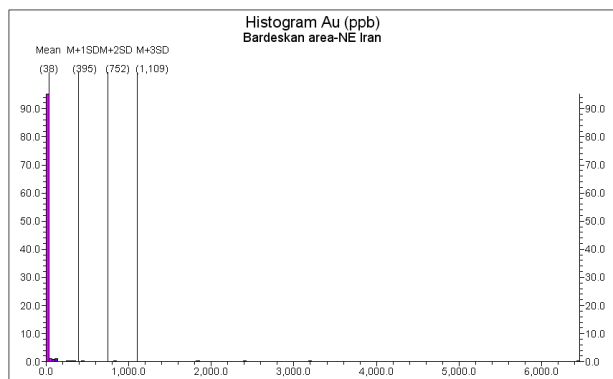


Fig. 3. Au, Cu, As and Sb in Bardaskan area

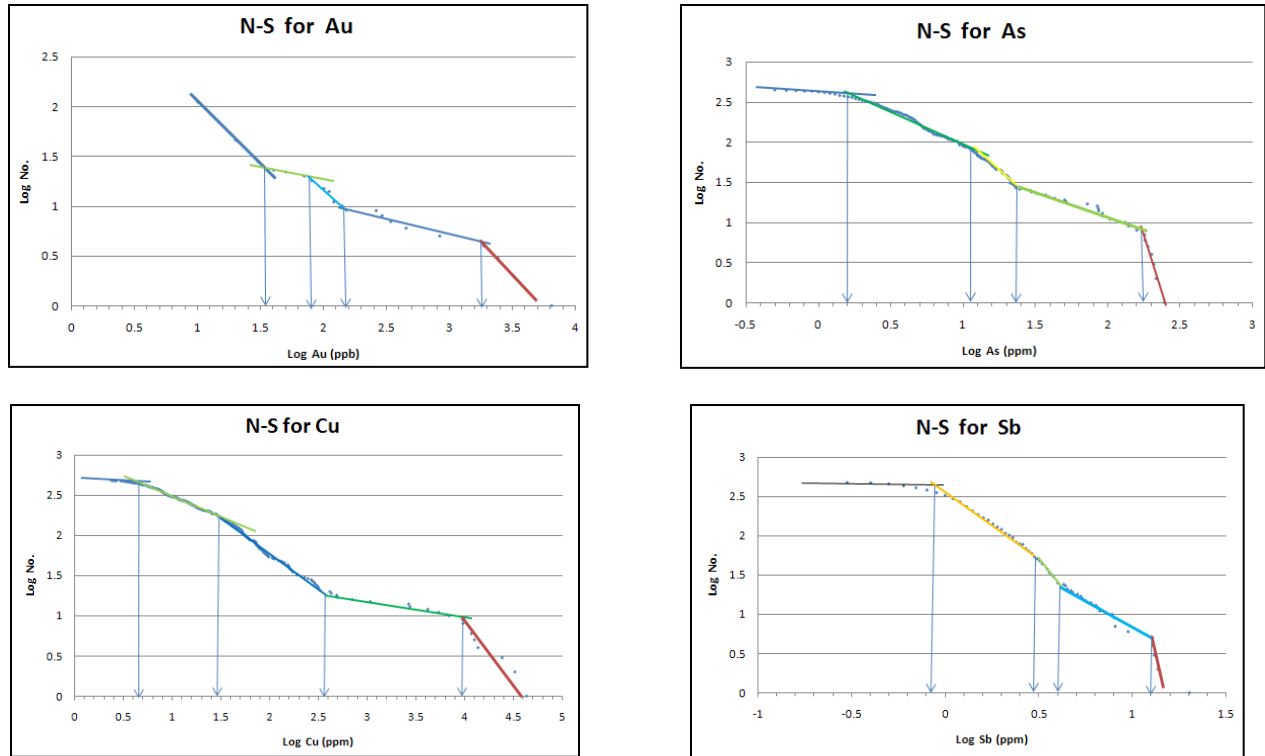


Figure 4. Log-log plots resulted from N-S model for Au, Cu, As and Sb.

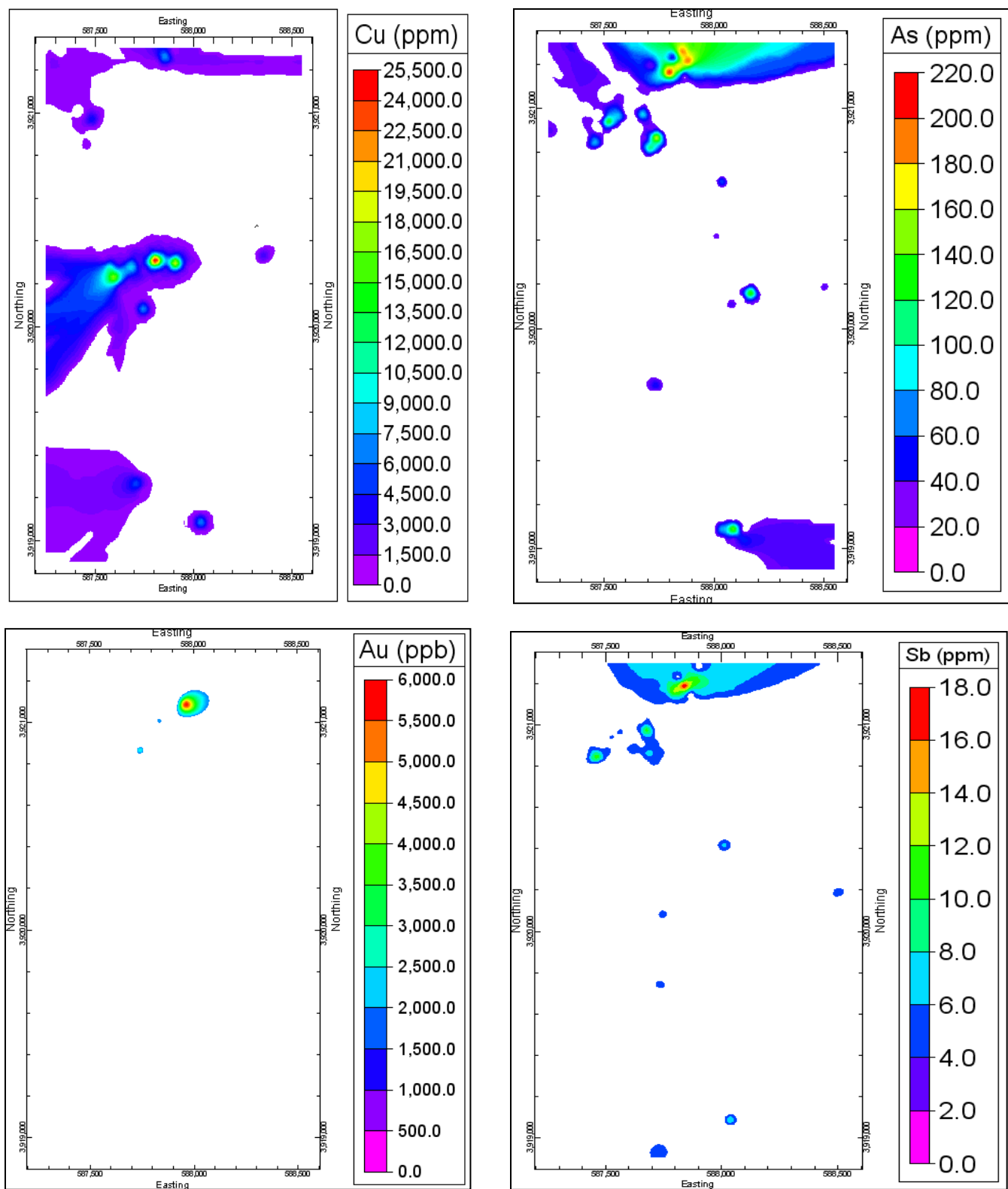


Fig. 5. Au, Cu, As and Sb geochemical population distribution maps based on N-S model

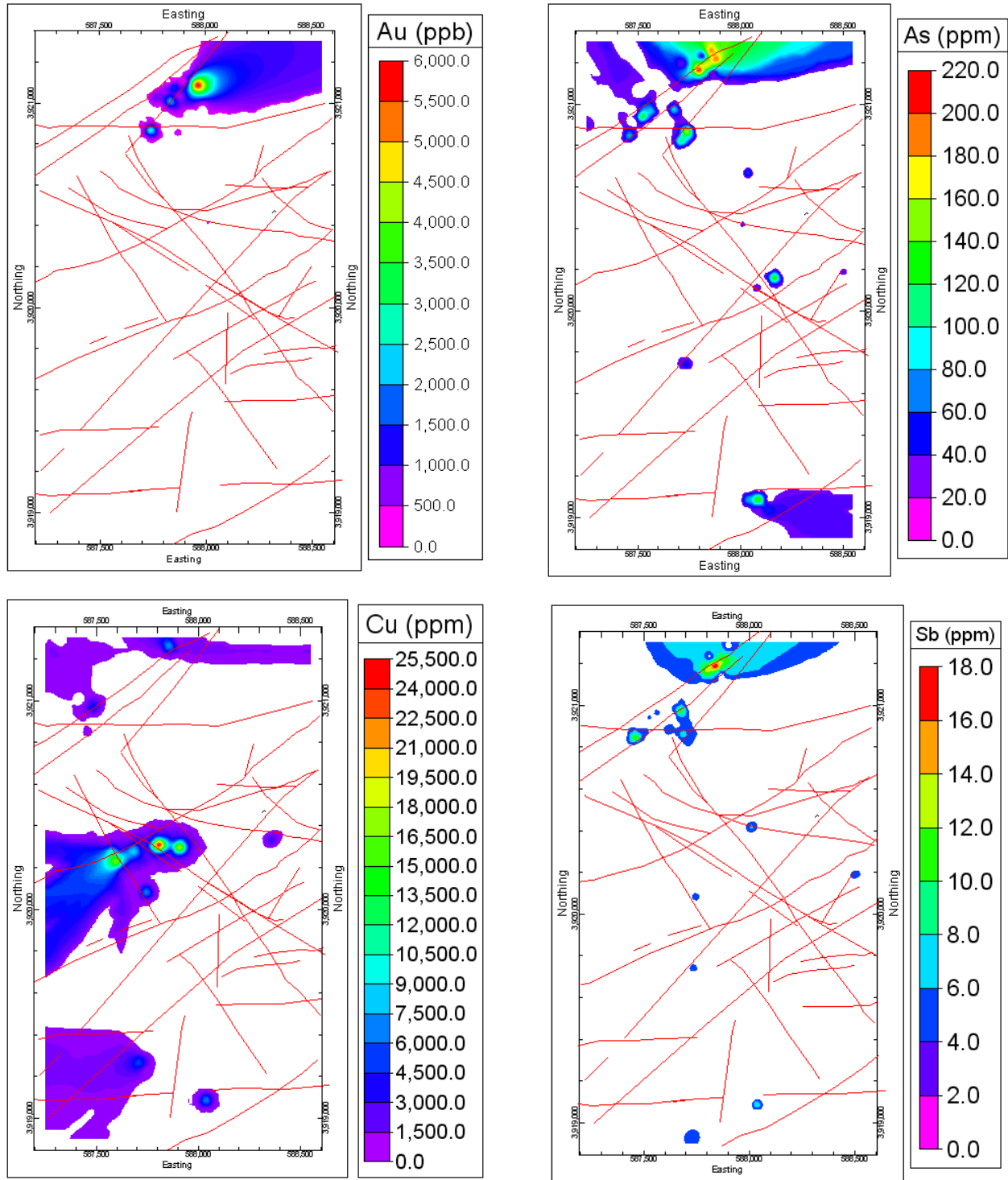


Fig. 6. Elemental geochemical population distribution maps based on N-S model imposed on fault location

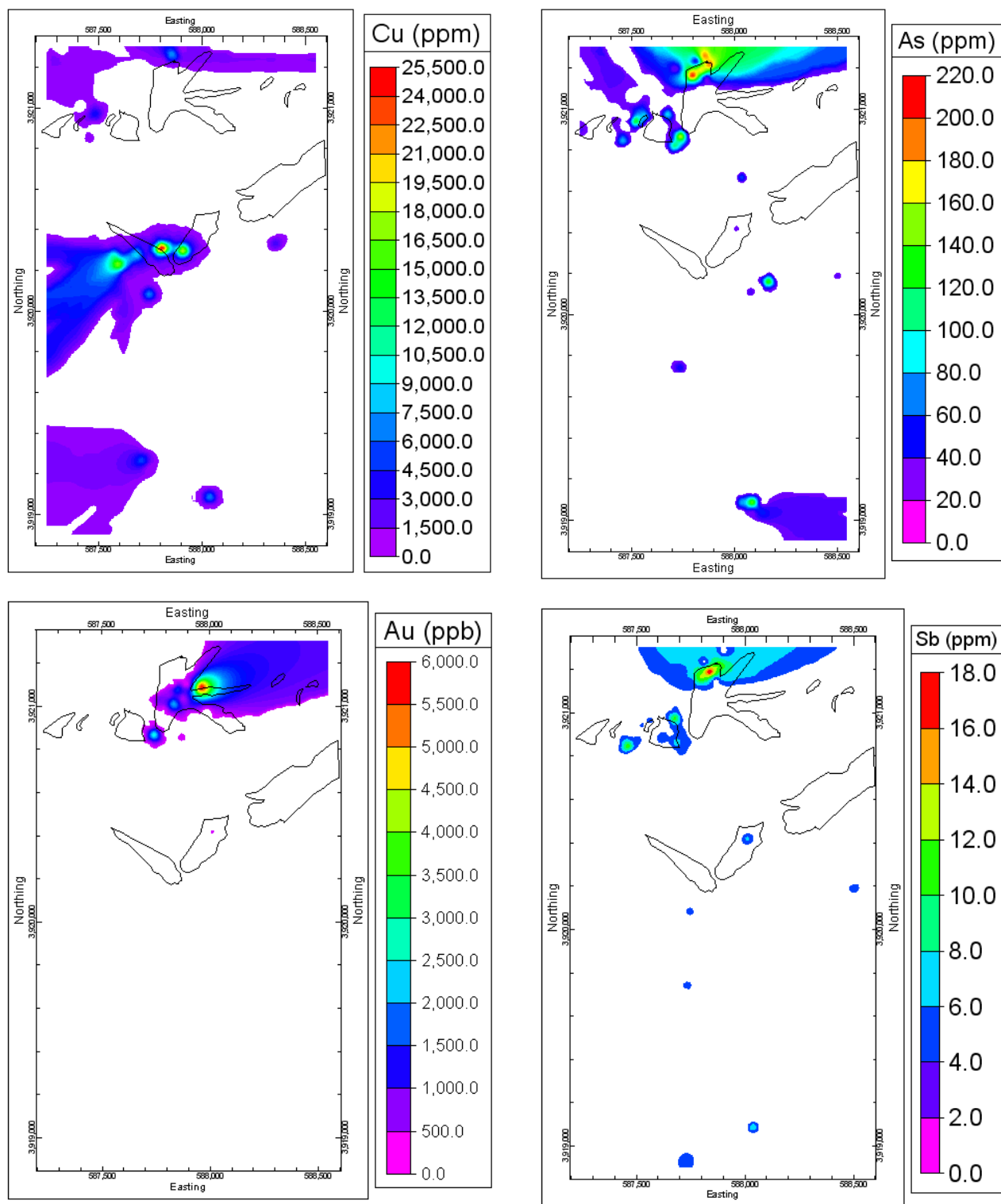


Fig. 7. Relationship between Au, Cu, As and Sb distribution and chloritization, phyllic and silicification alterations and sulfide mineralization (polygons)